Forecasting Research

Met O 11 Technical Note No. 9

A Comparison of Alternating Direction Implicit Methods for Solving the 3-D Semi-Geostrophic Equations on a Sphere

by

M.H. Mawson

May 1988

Me O 11)
London Road, 12 2SZ, England

MET O 11

TECHNICAL NOTE No 9

A Comparison of Alternating Direction Implicit Methods for Solving the 3-D Semi-Geostrophic Equations on a Sphere

M. H. Mawson

LONDON, METEOROLOGICAL OFFICE.
Met.O.11 Technical Note (New Series) No.9

A comparison of alternating direction implicity methods for solving the 3-D semi-geostrophic equations on a sphere.

08160688 FH2A

1. Introduction.

The semi-geostrophic equations have been shown to describe most motions of interest in weather forecasting, see for example Cullen, Norbury, Purser and Shutts (1987). The equations can be applied globally although their ability to predict atmospheric motion on a global scale for a period of days has yet to be proven. We consider using an implicit finite-difference scheme to solve the global equations. The method we use combines techniques developed by Meek and Norbury (1984) and Cohn et al (1985). This approach leads to the need to be able to solve large sparse matrix systems efficiently. The ease in which the equations can be split into x-z and y-z slices lends them to solution by an Alternating Direction Implicit (A. D. I.) method. In this note we concern ourselves with finding the optimum strategy for their solution by this method. Various schemes are presented along with the motivation behind them. They are then all applied to the same idealised test problem and their rates of convergence compared.

2. The Equations to be Solved.

The dry semi-geostrophic equations in spherical polar co-ordinates (λ, μ) are as follows:

$$p_* \frac{\partial u_\sigma}{\partial t} + \frac{1}{a\cos\mu} U \frac{\partial u_\sigma}{\partial \lambda} + \frac{V}{a} \frac{\partial u_\sigma}{\partial \mu} + S \frac{\partial u_\sigma}{\partial \sigma} - f(V - p_* v_\sigma) - \frac{U v_\sigma}{a} \tan\mu = F_u \qquad (1)$$

$$p_* \frac{\partial v_\sigma}{\partial t} + \frac{1}{a\cos\mu} U \frac{\partial v_\sigma}{\partial \lambda} + \frac{V}{a} \frac{\partial v_\sigma}{\partial \mu} + S \frac{\partial v_\sigma}{\partial \sigma} + f(U - p_* u_\sigma) + \frac{U u_\sigma}{a} \tan\mu = F_v \qquad (2)$$

$$p_* \frac{\partial \theta}{\partial t} + \frac{1}{a\cos\mu} U \frac{\partial \theta}{\partial \lambda} + \frac{V}{a} \frac{\partial \theta}{\partial \mu} + S \frac{\partial \theta}{\partial \sigma} = H \qquad (3)$$

$$\frac{\partial p_*}{\partial t} + \frac{1}{a\cos\mu} \left[\frac{\partial U}{\partial \lambda} + \frac{\partial}{\partial \mu}(V\cos\mu) \right] + \frac{\partial S}{\partial \sigma} = 0 \qquad (4)$$

$$f u_\sigma = -\frac{1}{a} \frac{\partial \phi}{\partial \mu} - \frac{1}{a} C_p \sigma^\kappa \theta \frac{\partial \pi}{\partial \mu} \qquad (5)$$

$$f v_\sigma = \frac{1}{a\cos\mu} \left[\frac{\partial \phi}{\partial \lambda} + C_p \sigma^\kappa \theta \frac{\partial \pi}{\partial \lambda} \right] \qquad (6)$$

$$-R\sigma^{\kappa-1}\,\pi\,\theta = \frac{\partial\phi}{\partial\sigma}\ ;\ \pi = (p_*/1000)^{\kappa}\ ,\ \kappa = R/C_p\ ,\ \sigma = p/p_* \qquad (7)$$

The boundary condition is S=0 at σ=0, 1.

Elimination of ϕ between (5), (6), and (7) gives

$$f\frac{\partial u_\Box}{\partial\sigma} = \frac{\pi R\sigma^{\kappa-1}}{a}\frac{\partial\theta}{\partial\mu} - \frac{1}{a}C_p\,\sigma^{\kappa}\frac{\partial\theta}{\partial\sigma}\frac{\partial\pi}{\partial\mu} \qquad (8)$$

$$f\frac{\partial v_\Box}{\partial\sigma} = \frac{1}{a\cos\mu}\left[-\pi R\sigma^{\kappa-1}\frac{\partial\theta}{\partial\lambda} + C_p\,\sigma^{\kappa}\frac{\partial\theta}{\partial\sigma}\frac{\partial\pi}{\partial\lambda}\right] \qquad (9)$$

Equations (6) and (7) are applied at σ=1 with $\phi = \phi_*(\lambda, \mu)$. The notation is standard, except that (U, V, S) represent (p_*u, p_*v, $p_*\dot{\sigma}$). H represents a source term for potential temperature: F_u, F_v are friction terms.
The equations are stepped forward in time using a predictor/corrector method. Here we describe only with the corrector step. Starting with an initial balanced state defined such that if

$$DE_1 = fv_\Box - \frac{1}{a\cos\mu}\left[\frac{\partial\phi_*}{\partial\lambda} + C_p\sigma^{\kappa}\theta_*\frac{\partial\pi}{\partial\lambda}\right] \qquad (10)$$

$$DE_k\ (2\leq k\leq N) = f\frac{\partial v_\Box}{\partial\sigma} + \frac{1}{a\cos\mu}\left[\pi R\sigma^{\kappa-1}\frac{\partial\theta}{\partial\lambda} - C_p\sigma^{\kappa}\frac{\partial\theta}{\partial\sigma}\frac{\partial\pi}{\partial\lambda}\right] \qquad (11)$$

$$DN_1 = fu_\Box + \frac{1}{a}\left[\frac{\partial\phi_*}{\partial\mu} + C_p\sigma^{\kappa}\theta_*\frac{\partial\pi}{\partial\mu}\right] \qquad (12)$$

$$DN_k\ (2\leq k\leq N) = f\frac{\partial u_\Box}{\partial\sigma} - \frac{1}{a}\left[\pi R\sigma^{\kappa-1}\frac{\partial\theta}{\partial\mu} - C_p\sigma^{\kappa}\frac{\partial\theta}{\partial\sigma}\frac{\partial\pi}{\partial\mu}\right] \qquad (13)$$

then DE_k $(1\leq k\leq N) = 0$ and DN_k $(1\leq k\leq N) = 0$ and then perturb it so that the DE_k's and/or the DN_k's are no longer zero. To return the model to a balanced state we solve the following:

$$f\Delta v_\Box - \frac{1}{a\cos\mu}C_p\sigma^{\kappa}\left[\Delta\theta_*\frac{\partial\pi}{\partial\lambda} + \theta_*\kappa\frac{\partial}{\partial\lambda}\left(\pi\frac{\Delta p_*}{p_*}\right)\right] = -DE_1 \qquad (14)$$

$$f\frac{\partial\,\Delta v_\Box}{\partial\sigma} + \frac{1}{a\cos\mu}\left[\kappa R\sigma^{\kappa-1}\frac{\Delta p_*}{p_*}\frac{\partial\theta}{\partial\lambda} + \pi R\sigma^{\kappa-1}\frac{\partial\Delta\theta}{\partial\lambda}\right.$$

$$\left. - C_p\sigma^{\kappa}\frac{\partial\Delta\theta}{\partial\sigma}\frac{\partial\pi}{\partial\lambda} - \kappa C_p\sigma^{\kappa}\frac{\partial\theta}{\partial\sigma}\frac{\partial}{\partial\lambda}\left(\pi\frac{\Delta p_*}{p_*}\right)\right] = -DE_k\ (2\leq k\leq N)$$

$$f\Delta u_{\lambda} + \frac{1}{a}\left[C_p\sigma^{\kappa} \left(\Delta\theta \frac{\partial\pi}{\partial\mu} + \theta_* \kappa \frac{\partial}{\partial\mu} \left(\frac{\pi\Delta p_*}{p_*} \right) \right) \right] = - DN_1 \qquad (16)$$

$$f \frac{\partial\Delta u_{\lambda}}{\partial\sigma} - \frac{1}{a}\left[\frac{\kappa R\sigma^{\kappa-1}\pi\, \Delta p_*}{p_*} \frac{\partial\theta}{\partial\mu} + \pi R\sigma^{\kappa-1} \frac{\partial\Delta\theta}{\partial\mu} \right. \qquad (17)$$

$$\left. - C_p\sigma^{\kappa} \frac{\partial\Delta\theta}{\partial\sigma} \frac{\partial\pi}{\partial\mu} - \kappa C_p\sigma^{\kappa} \frac{\partial\theta}{\partial\sigma} \frac{\partial}{\partial\mu} \left(\frac{\pi\Delta p_*}{p_*} \right) \right] = - DN_k \quad (2 \leq k \leq N)$$

To simplify the solution of equations 14-15 and 16-17 we introduce stream-functions as follows:

for equations 14-15 consider the continuity equation (4) on an east-west slice

$$\frac{\partial p_*}{\partial t} + \frac{1}{a\cos\mu} \frac{\partial U}{\partial\lambda} + \frac{\partial S}{\partial\sigma} = 0 \qquad (18)$$

Taking the vertical mean of this yields

$$\frac{\partial p_*}{\partial t} + \frac{1}{a\cos\mu} \frac{\partial\tilde{U}}{\partial\lambda} = 0 \qquad (19)$$

where $\tilde{U}$ denotes the vertical mean of U.

Subtracting 19 from 18 gives

$$\frac{1}{a\cos\mu} \frac{\partial}{\partial\lambda} (U-\tilde{U}) + \frac{\partial S}{\partial\sigma} = 0 \qquad (20)$$

so we can define a stream-function ψ such that

$$- \frac{\partial\psi}{\partial\sigma} = U - \tilde{U} \qquad \text{and} \qquad \frac{\partial\psi}{\partial\lambda} = S\, a\cos\mu \qquad (21)$$

The corrections $\Delta\theta$, Δp_*, Δv_{λ} in equations 14-15 can be written as follows:

$$p_*\frac{\Delta\theta}{\Delta t} + \frac{1}{a\cos\mu} U \frac{\partial\theta}{\partial\lambda} + S\frac{\partial\theta}{\partial\sigma} = 0 \qquad (22)$$

$$\frac{\Delta p_*}{\Delta t} + \frac{1}{a\cos\mu} \frac{\partial\tilde{U}}{\partial\lambda} = 0 \qquad (23)$$

$$p_* \frac{\Delta v_{\lambda}}{\Delta t} + \frac{1}{a\cos\mu} U\frac{\partial v_{\lambda}}{\partial\lambda} + S\frac{\partial v_{\lambda}}{\partial\sigma} + f(U-p_*u_{\lambda}) = 0 \qquad (24)$$

We can now substitute for U and S in 22-24 using 21 and hence write the corrections in terms of ψ and $\tilde{U}$. To ensure a unique, numerically stable solution to these equations it is necessary to oust certain terms in 22 and 24 and also the terms in $\Delta\theta$ in 14 and the terms in Δp_* and $\partial/\partial\sigma\ \Delta\theta$ in 15 as explained in Cullen (1988). It is also necessary to adjust the fields to satisfy a stability criterion before the equations are solved. These omissions are equivalent to under-relaxation and means that extra iterations may be needed to reduce the residuals by a given amount.

22 becomes:

$$ap_*\cos\mu\ \frac{\Delta\theta}{\Delta t} + \frac{\partial\psi}{\partial\lambda}\frac{\partial\theta}{\partial\sigma} = 0 \qquad (25)$$

24 becomes:

$$p_*\frac{\Delta v_\Omega}{\Delta t} - \frac{1}{a\cos\mu}\frac{\partial v_\Omega}{\partial\lambda}\frac{\partial\psi}{\partial\sigma} - f\frac{\partial\psi}{\partial\sigma} + f\tilde{U} + \frac{\tilde{U}}{a\cos\mu}\frac{\partial v_\Omega}{\partial\lambda} = 0 \qquad (26)$$

with stability criterion:

$f(v_\Omega + fx)$ must be monotonic increasing in the positive x-direction and $\partial\theta/\partial\sigma > 0$.

Substituting 23, 25 and 26 into 14 and 15 gives a system of equations which is solved by the block tri-diagonal method described in Appendix B. The corrections $\Delta\theta$, Δp_*, and Δv_Ω are found by reapplying 25, 23 and 26 again respectively.

A similar argument is applied to equations 16-17 on a north-south slice. The analogous terms to those ignored in 14-15 , 22 and 24 are ignored in this slice with the stream-function defined by :

$$-\frac{\partial\psi}{\partial\sigma} = (V-\tilde{V})\cos\mu \qquad \text{and} \qquad \frac{\partial\psi}{\partial\mu} = Sa\cos\mu \qquad (27)$$

where $\tilde{V}$ denotes the vertical mean of V. The corrections to $\Delta\theta$, Δp_* and Δu_Ω are given by

$$ap_*\cos\mu\ \frac{\Delta\theta}{\Delta t} + \frac{\partial\psi}{\partial\mu}\frac{\partial\theta}{\partial\sigma} = 0 \qquad (28)$$

$$p_*\frac{\Delta u_\Omega}{\Delta t} - \frac{1}{a\cos\mu}\frac{\partial u_\Omega}{\partial\mu} - af\frac{\partial\psi}{\partial\sigma} + \frac{\tilde{V}}{a}\frac{\partial u_\Omega}{\partial\mu} - f\tilde{a} = 0 \qquad (29)$$

$$\frac{\Delta p_*}{\Delta t} + \frac{1}{a\cos\mu}\frac{\partial}{\partial\mu}(\tilde{V}\cos\mu) = 0 \qquad (30)$$

with the stability criterion that $f(-u_g + fy)$ must be monotonic increasing in the positive y-direction and $\partial\theta/\partial\sigma > 0$.

When the corrections are calculated at the end of the east-west slice different strategies for their use before the north-south slice begins may be employed, similarly for the corrections arrived at at the end of the north-south slice. Various alternatives are described in the next section. The solution of east-west then north-south slices is iterated until the residuals are removed. The correction strategies are discussed in the next section. The discretisation of the equations is described in Cullen and Mawson (1987) and the grid used is illustrated in Appendix A.

3. A.D.I Strategies.

i) Normal.

This is the control run with the full correction applied at the end of each slice.

Procedure:

East-west slice update:

$$\theta_k = \theta_k + \Delta\theta_k \qquad 2 \leq k \leq N$$
$$p_* = p_* + \Delta p_*$$
$$v_{gk} = v_{gk} + \Delta v_{gk} \qquad 1 \leq k \leq N$$

North-south slice update:

$$\theta_k = \theta_k + \Delta\theta_k \qquad 2 \leq k \leq N$$
$$p_* = p_* + \Delta p_*$$
$$u_{gk} = u_{gk} + \Delta u_{gk} \qquad 1 \leq k \leq N$$

ii) Delayed:

Here no correction is applied to θ and p_* at the end of the East-west slice but is remembered and applied at the end of the North-south slice.

Procedure:

East-west slice update:

store $\Delta\theta_{Ek}$
store Δp_{*E}
$$v_{gk} = v_{gk} + \Delta v_{gk} \qquad 1 \leq k \leq N$$

North-south slice update:

$$\theta_k = (\Delta\theta_{Ek} + \Delta\theta_{Nk})/2 + \theta_k \qquad 2 \leq k \leq N$$
$$p_* = (\Delta p_{*E} + \Delta p_{*N})/2 + p_*$$
$$u_{gk} = u_{gk} + \Delta u_{gk} \qquad 1 \leq k \leq N$$

The motivation behind trying this is as follows :
Suppose $\Delta\theta_{Ek} = \Delta\theta_{Nk}$ and $\Delta p_{*E} = \Delta p_{*N}$ then $DE_k = 0$, $DN_k = 0$ for all k and we have removed all the residual in one iteration. However if we had used method (i) then this solution would have taken more iterations to arrive at.

iii) Relaxed θ and p_* approach.

This version is the same is i) except that instead of applying the full correction to θ and p_* at the end of each slice α times it is applied with $0 \leq \alpha \leq 1$.

4. Problem posed.

Consider a uniform, stably stratified fluid at rest above a sphere with no orography. A perturbation is introduced by redefining the surface pressure in a particular area and calculating a consistent φ_* using 5 or 6 but not altering the potential temperature or velocity fields . This can be considered as growing a mountain in the fluid. The mountain is specified such that it is symmetrical.

5. Model Solution.

The problem described above was solved on a 3 x 3.75 degree grid with 11 levels in the vertical which were almost .equally spaced. The mountain covered 20 grid-lengths from corner to corner with a mountain top pressure of 920 mb initially, chosen so that none of the ADI schemes needed to call the routines which adjust the geostrophic wind and potential temperature fields to ensure the stability criterions are satisfied. These routines are described in Cullen and Mawson (1987). The mountain was placed so that the top was at 45 N . Figure 1 shows the plan view of the mountain along with the lines of the cross-sections taken through it.

The cold dense air originally at the top of the mountain flows down the sides as can be seen in the sequence of figures 2-4. This flow is deflected by the Coriolis effect and a circulation characteristic of a high pressure vortex is set up with subsidence above the mountain and an anti-cyclonic circulation at the surface. To balance the outflow at the surface there is a corresponding inflow aloft and associated cyclonic vortex due to coriolis effect. This can be seen in the wind component cross-sections, figures 5-12.

These figures are taken from runs using ADI scheme (i) and the behaviour of it can be clearly seen. At time-step 1 the East-west slice removes all its residual producing a modified potential temperature field which is close to the final one. However the North-south slice still sees a large residual and also produces a change to the temperature field in the same sense as the East-west slice. Now the East-west slice sees a residual of the opposite sign to before and corrects the potential temperature in the opposite direction to the first time-step. The north-south slice now sees a residual of the same sign as its first time-step and so corrects tthe field accordingly.

Schematically:

	Time-step	θ	$u_\square$	$v_\square$
E-W	1	+		+
N-S	1	+	+	
E-W	2	-		-
N-S	2	+	+	

where the (+,-) denote the increase or decrease of the quantity implied by the solver.

This can be seen happening in the model by comparing the wind components after 1 and 5 time-steps. u_3 time-step 1 is in figures 5 and 9 and the corresponding v_3 in 6 and 10, the 5 time-step u_3 is in figures 7 and 11 with v_3 in 8 and 12. Trying to remove this oscillation was the motivating idea of scheme (ii) whilst scheme (iii) was an attempt to damp it to see if that would improve convergence.

6. Comparison of schemes.

The three schemes were all applied to the problem and the following measure of their convergence rates was compared.

$$\hat{V} = \Sigma_i |V_i|$$

where V is the implied correction at sigma level 4 in the North-south slice summed over 15 points from the top of the mountain northwards. The graph of $\hat{V}$ against number of time-steps is shown in figure 13. The graph for scheme (iii) is with the parameter $\alpha = 0.7$ which provided the best result. The difference between this line and that of the control scheme (i) is small and choice of which approach to use is not obvious. Scheme (ii) is worse than the other two and this is due to the assumption about the temperature corrections being equal from both slices being untrue. A possible way to decide between schemes (i) and (iii) is to run them with the mountain placed at the equator. This will be invesigated in conjunction with other work studing the models behaviour in the tropics.

7. Conclusion.

The ADI approach is a practical method for solving the corrector step of this scheme although there appears to be more than one variant capable of solving a problem with similar efficiency. It is hoped that a clearer indication of which to use may be gained later and furthur variants which may possibly be more efficient will be tried if and when they come to light.

Appendix A.

The variables are staggered in space as follows :

E-W Slice

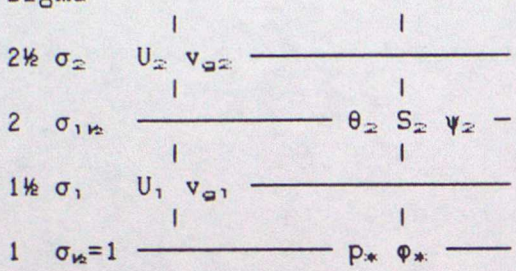

N-S Slice

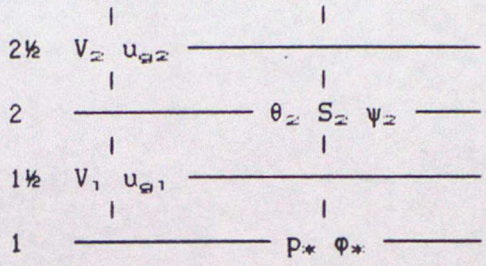

Assume that there are N levels in the vertical, the upper boundary corresponds to the Nth θ point.

Horizontal Arrangement.

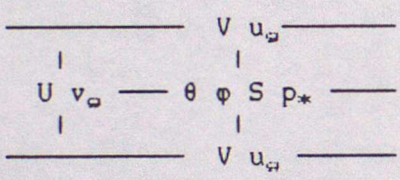

N. Pole

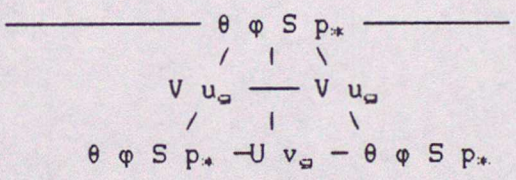

The data is arranged to be doubly periodic in the horizontal. The finite-difference scheme is fully implicit in time and centred in space.

Appendix B. Solution of slice equations.

The method applies equally to latitudinal and longitudinal slices since the data has been arranged to appear doubly periodic. In both situations the equations take the form

$$Cu_{x-\Delta x} + Au_x + Bu_{x+\Delta x} = f \qquad (A1)$$

where capitals denote a matrix and lower case a vector. A, B, C are NxN and u, f are of length N with A1 periodic.

Assume the points in the x-direction are numbered 1 to L. The cyclic system is solved by combining a non-cyclic algorithm for points 1 to (L-1) with a special procedure for point L.

The procedure is then divided into the following stages.

a) Forward sweep.

$$\tilde{A}_1 = A_1 \ , \ \tilde{G}_1 = C_1 \qquad (A2)$$

$$\tilde{f}_1 = f_1$$

$$G_i = 0 \ , \ 2 \leq i \leq L-2 \qquad (A3)$$

$$G_{L-1} = B_{L-1}$$

$$\tilde{A}_{i+1} = A_{i+1} - C_{i+1}\,\tilde{A}_i^{-1}\,B_i \qquad 1 \leq i \leq L-2 \qquad (A4a)$$

$$\tilde{f}_{i+1} = f_{i+1} - C_{i+1}\,\tilde{A}_i^{-1}\,\tilde{f}_i \qquad 1 \leq i \leq L-2 \qquad (A4b)$$

$$\tilde{G}_{i+1} = G_{i+1} - C_{i+1}\,\tilde{A}_i^{-1}\,\tilde{G}_i \qquad 1 \leq i \leq L-2 \qquad (A4c)$$

b) Solution of equations at end point.

$$v_{L-1} = \tilde{A}_{L-1}^{-1}\,\tilde{f}_{L-1} \qquad (A5)$$

$$D_{L-1} = \tilde{A}_{L-1}^{-1}\,\tilde{G}_{L-1}$$

c) Back substitution.

$$v_i = \tilde{A}_i^{-1}\,(\,\tilde{f}_i - B_i\,v_{i+1}\,) \qquad L-2 \geq i \geq 1 \qquad (A6)$$

$$D_i = \tilde{A}_i^{-1}\,(\tilde{G}_i - B_i\,D_{i+1}\,) \qquad L-2 \geq i \geq 1$$

d) Solve for Lth point.

$$(\,A_L - B_L\,D_1 - C_L\,D_{L-1}\,)u_L = f_L - B_L\,v_1 - C_L\,v_{L-1} \qquad (A7)$$

e) Correct other points.

$$u_i = v_i - D_i\,u_L \qquad 1 \leq i \leq L-1 \qquad (A8)$$

References.

Cullen M.J.P, Norbury J, Shutts G.J, Purser R.J, 1987
Modelling the Quasi-equilibrium dynamics of the atmosphere.
Quart. J. Roy. Meteor. Soc. 113 pp735-757

Meek P.C, Norbury J, 1984
Nonlinear moving boundary problems and a Keller box scheme.
SIAM J Numer Anal 21 pp883-893

Cohn S.E, Dee D, Isaacson E, Marchesin D, Zwas G, 1985
A fully implicit scheme for the Barotropic Primitive equations.
Mon Weath Rev 113 pp436-448

Cullen M.J.P 1988
Implicit finite-difference methods for computing discontinuous atmospheric flows.
(submitted to J. Comp. Phys.)

Cullen M.J.P, Mawson M.H 1987
A fully implicit scheme for the 3-D Quasi-Equilibrium equations.
(internal branch working paper N° 85 copy available in Met o.11)

List of Figures.

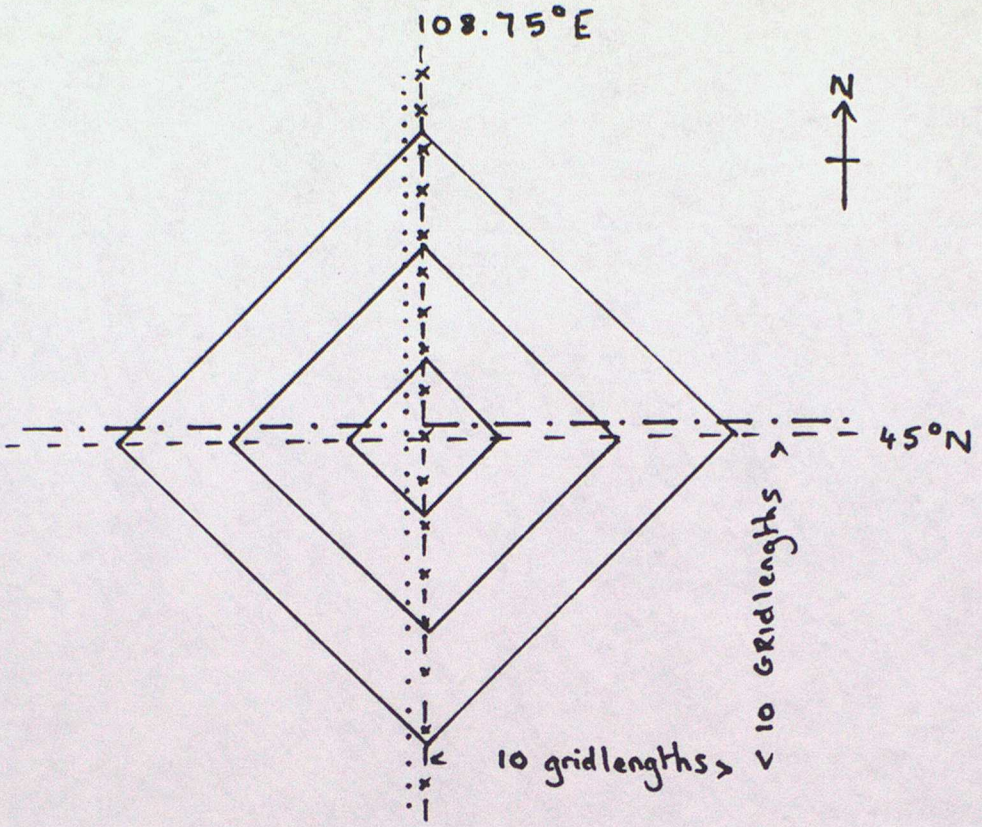

FIGURE 1, Plan View of Mountain,

Solid lines are contours of orography,

— — — — — is the line of the East-west θ, v_g cross-sections,

—·—·—· is the line of the East-west u_g cross-section,

—x—x—x—x— is the line of the North-south θ, u_g cross-sections,

····· is the line of the North-south v_g cross-section,

FIGURE 2.

POTENTIAL TEMPERATURE

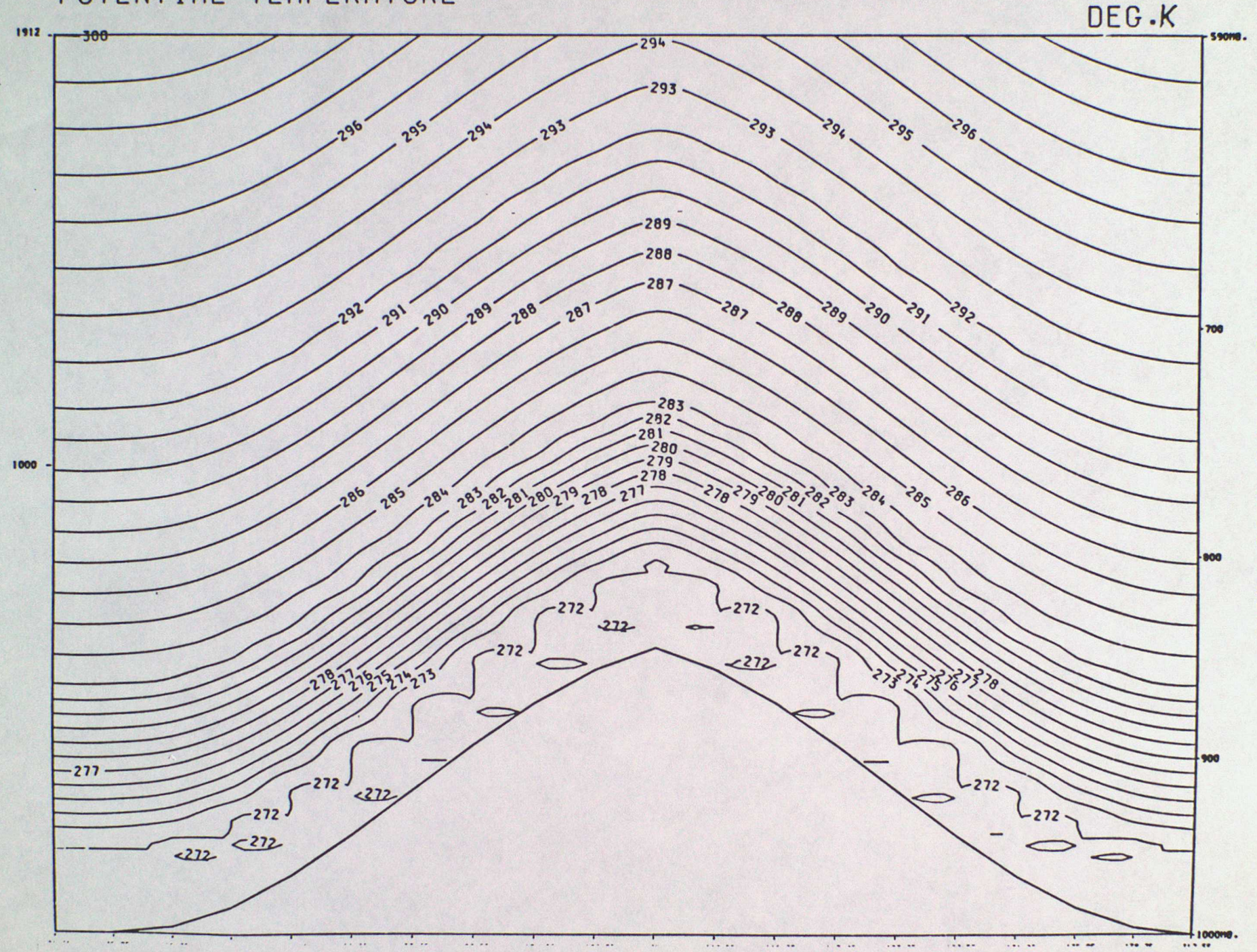

FIGURE 3

POTENTIAL TEMPERATURE

DEG.K

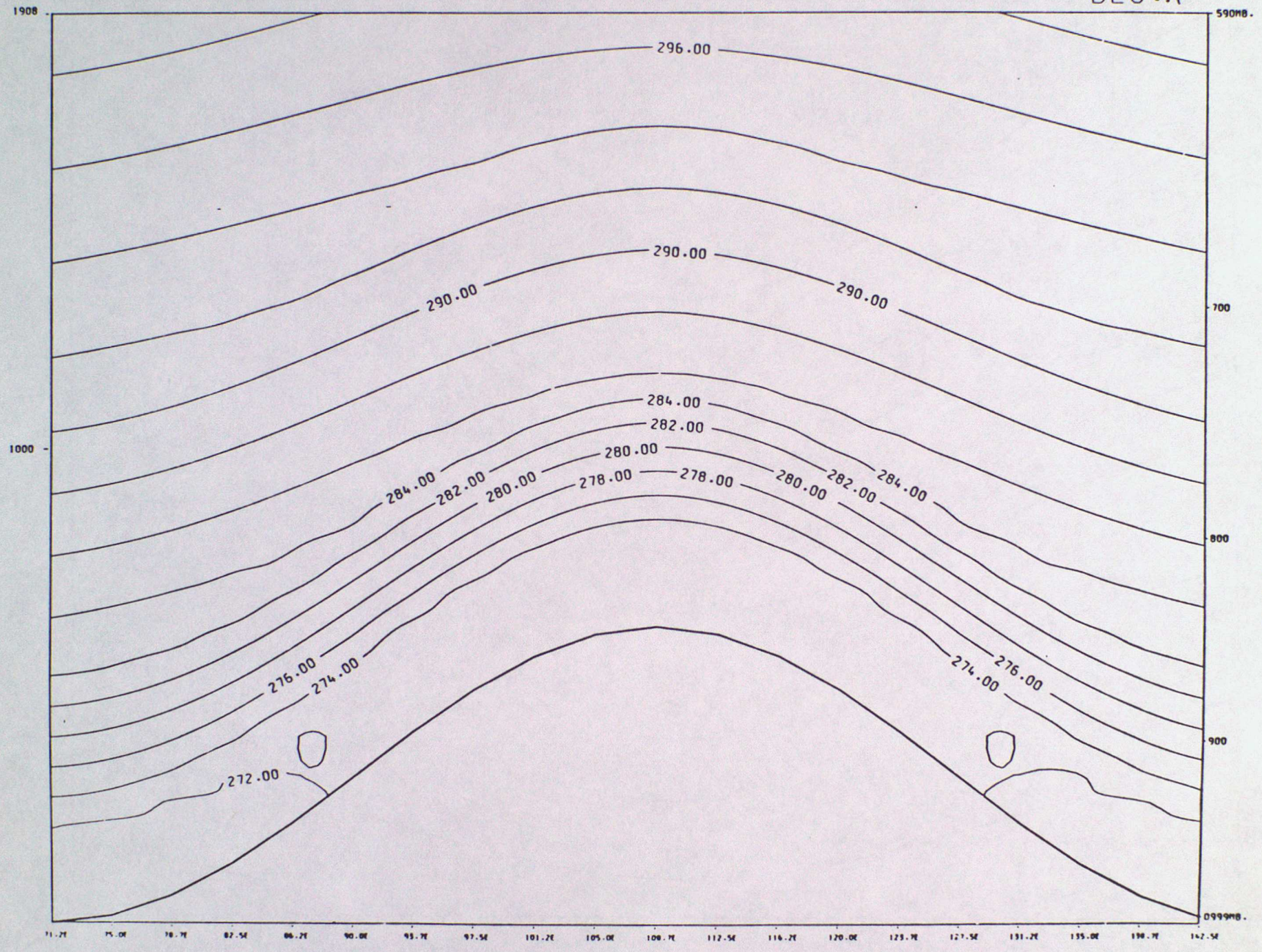

HEIGHT IN METRES

PRESSURE AT END GRID POINT

FIGURE 4

POTENTIAL TEMPERATURE

DEG.K

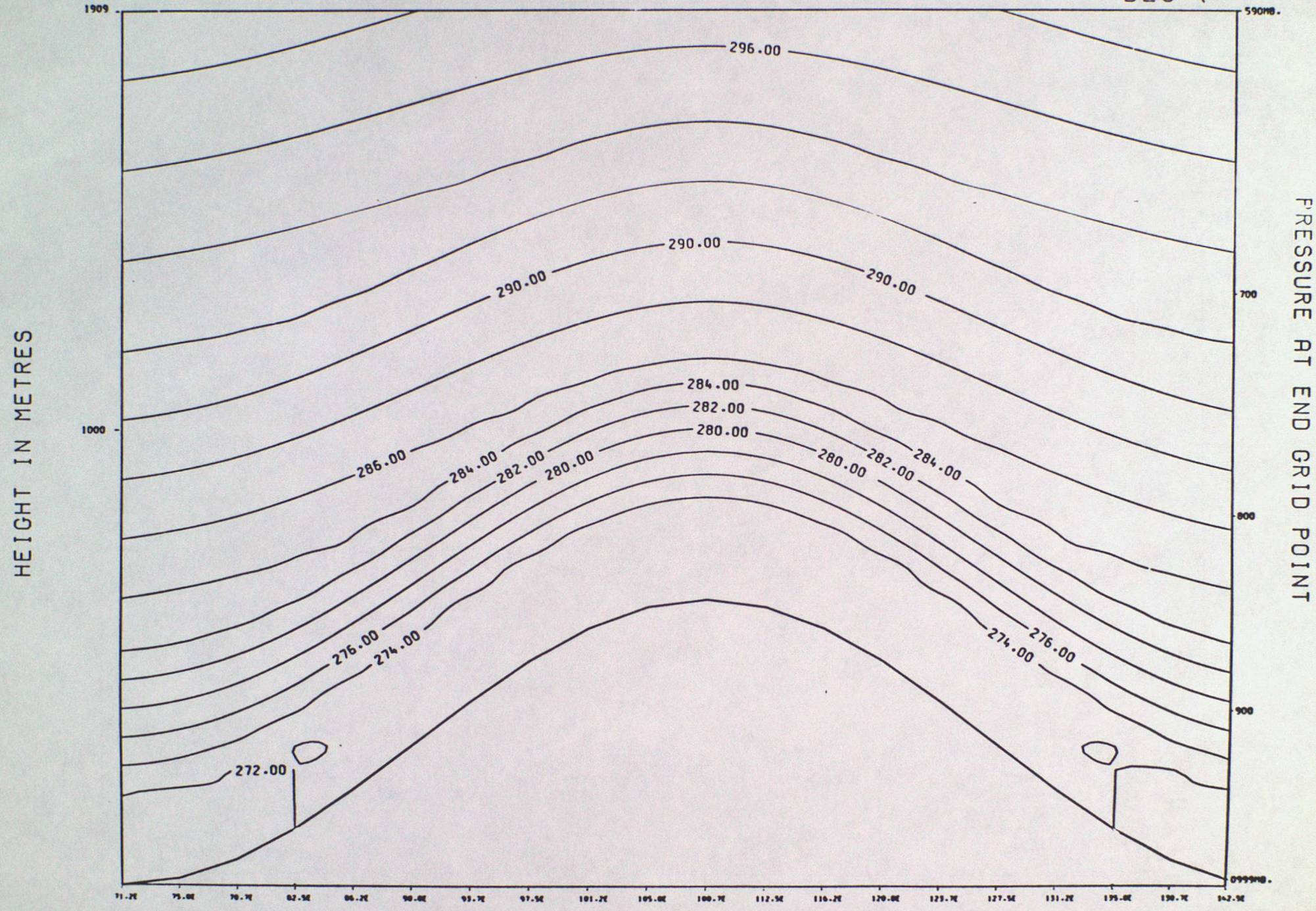

Figure. 5.

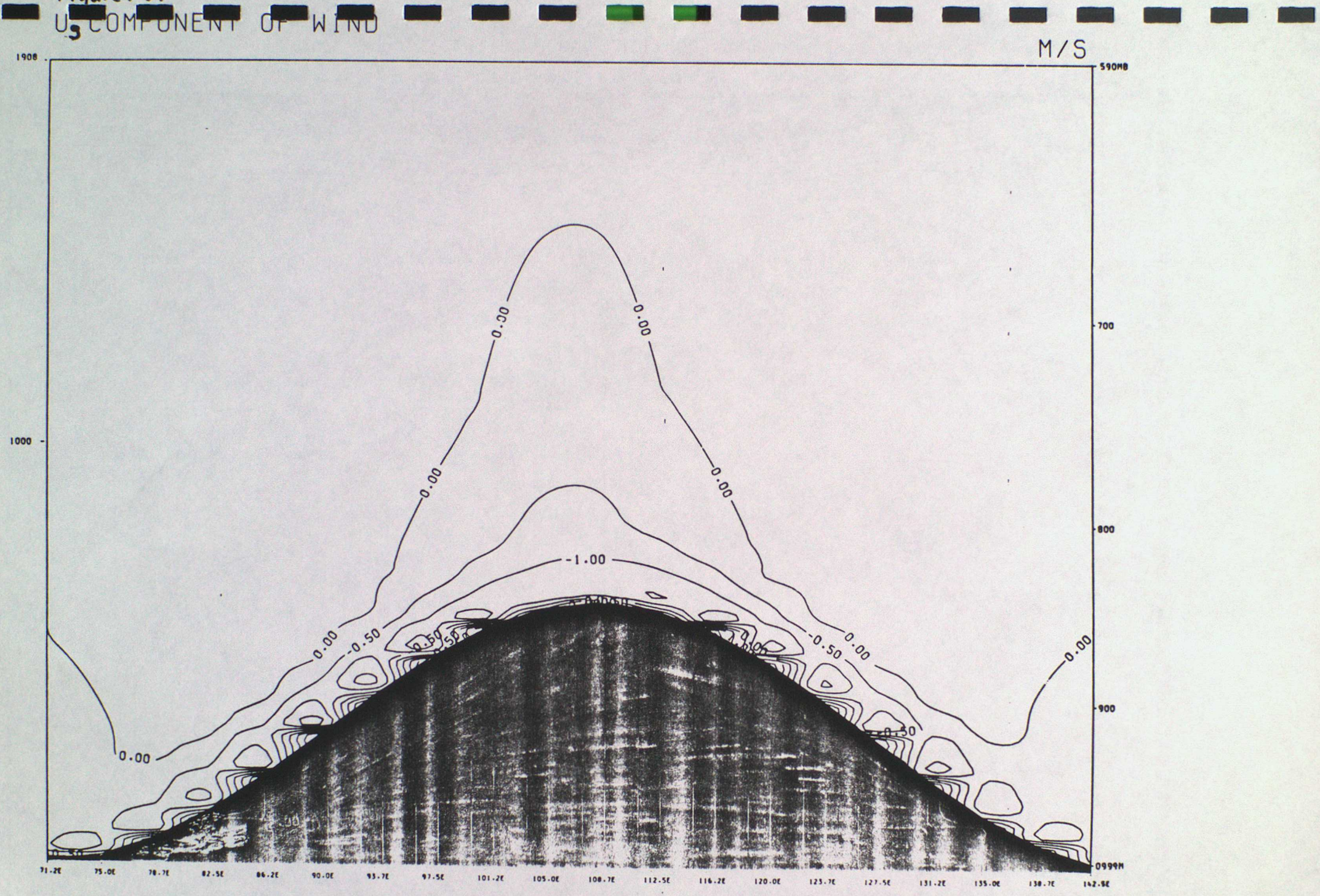
U3 COMPONENT OF WIND
M/S
1000
590MB
700
800
900
0999M
0.00
-0.50
-1.00
71.2E
75.0E
78.7E
82.5E
86.2E
90.0E
93.7E
97.5E
101.2E
105.0E
108.7E
112.5E
116.2E
120.0E
123.7E
127.5E
131.2E
135.0E
138.7E
142.5E
CROSS-SECTION ALONG LATITUDE 45.00N

Figure 6

V_g COMPONENT OF WIND

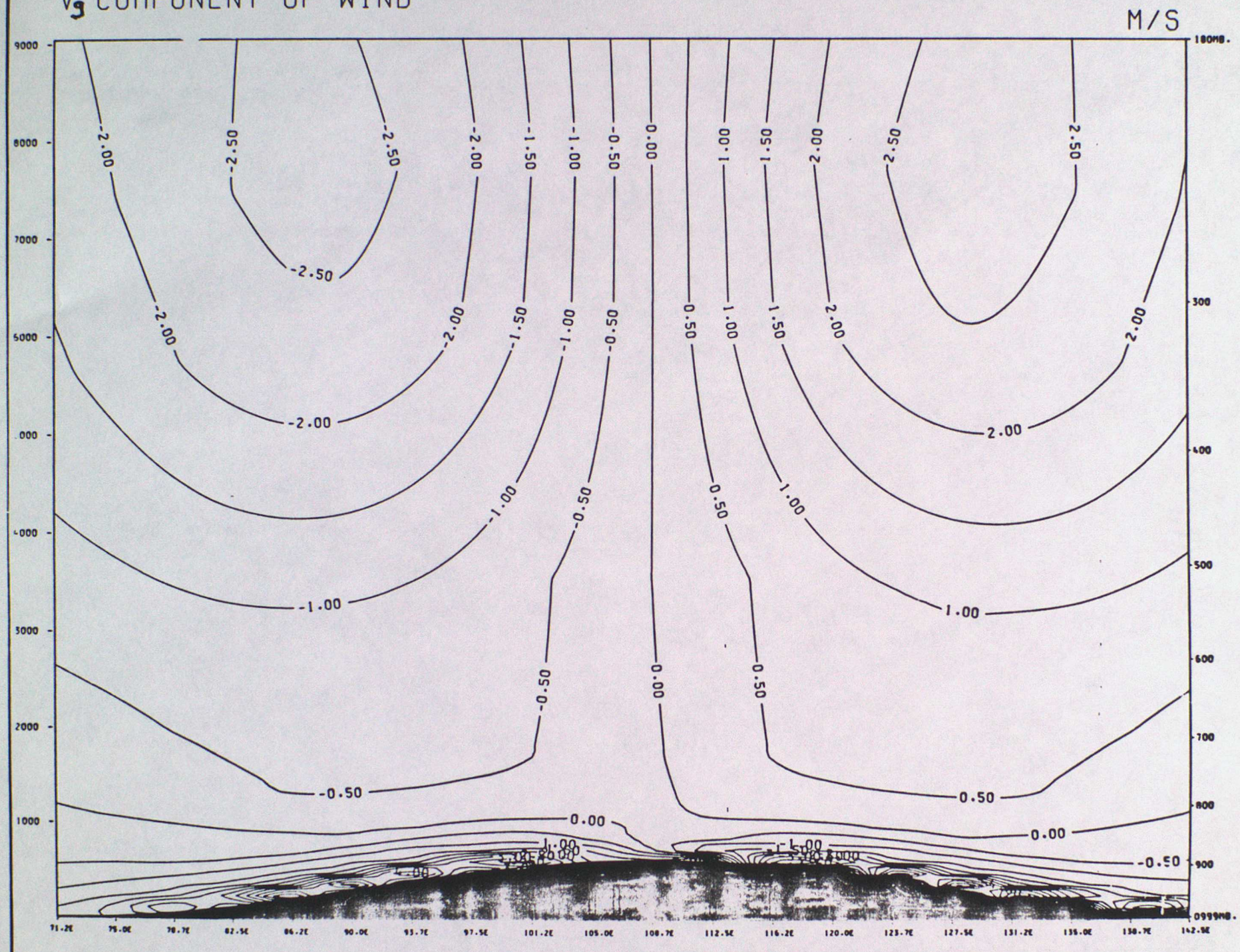

CROSS-SECTION ALONG LATITUDE 45.00N

Figure 7.

U COMPONENT OF WIND

M/S

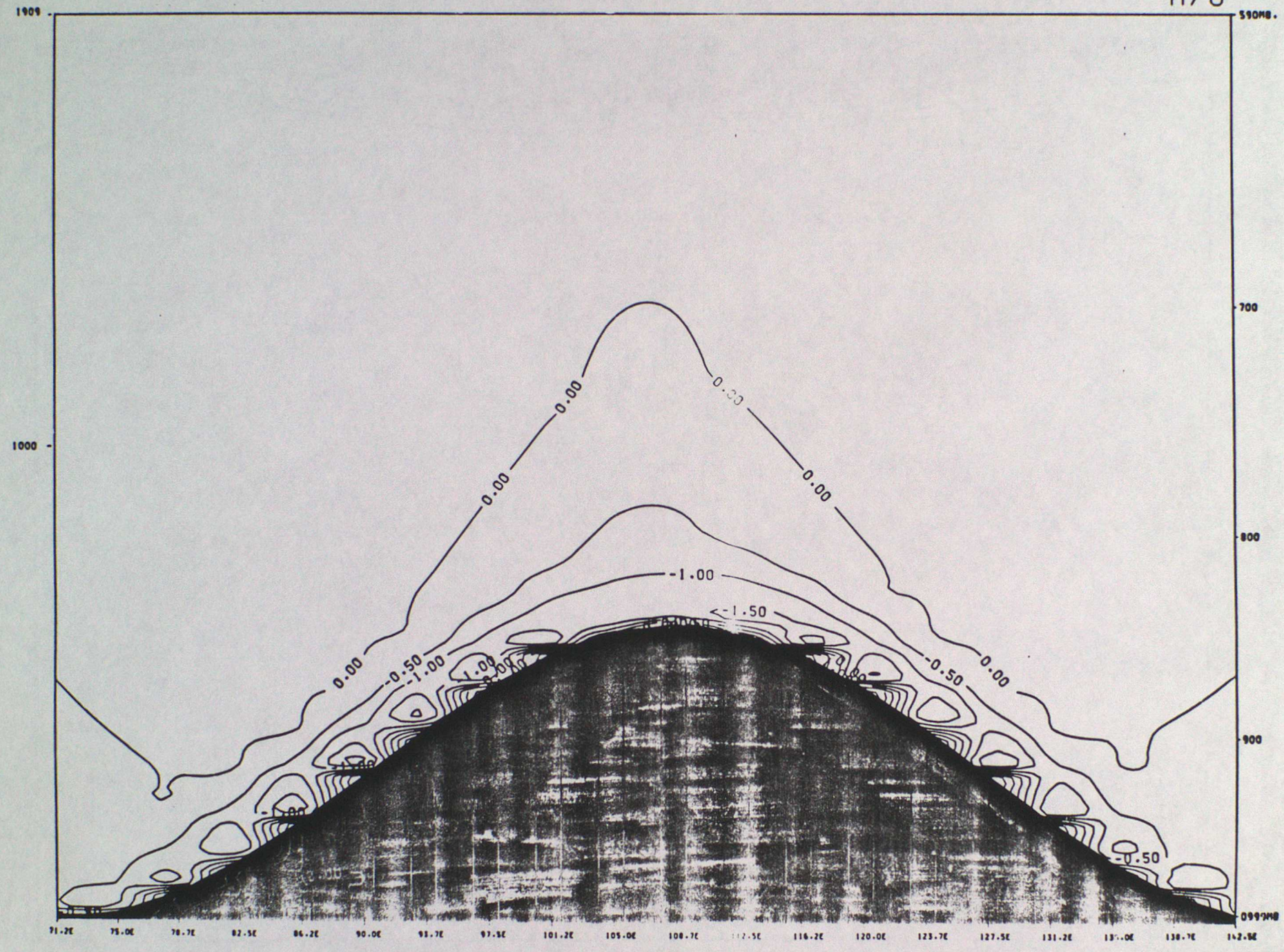

CROSS-SECTION ALONG LATITUDE 45.00N

Figure. 8.

V_S COMPONENT OF WIND

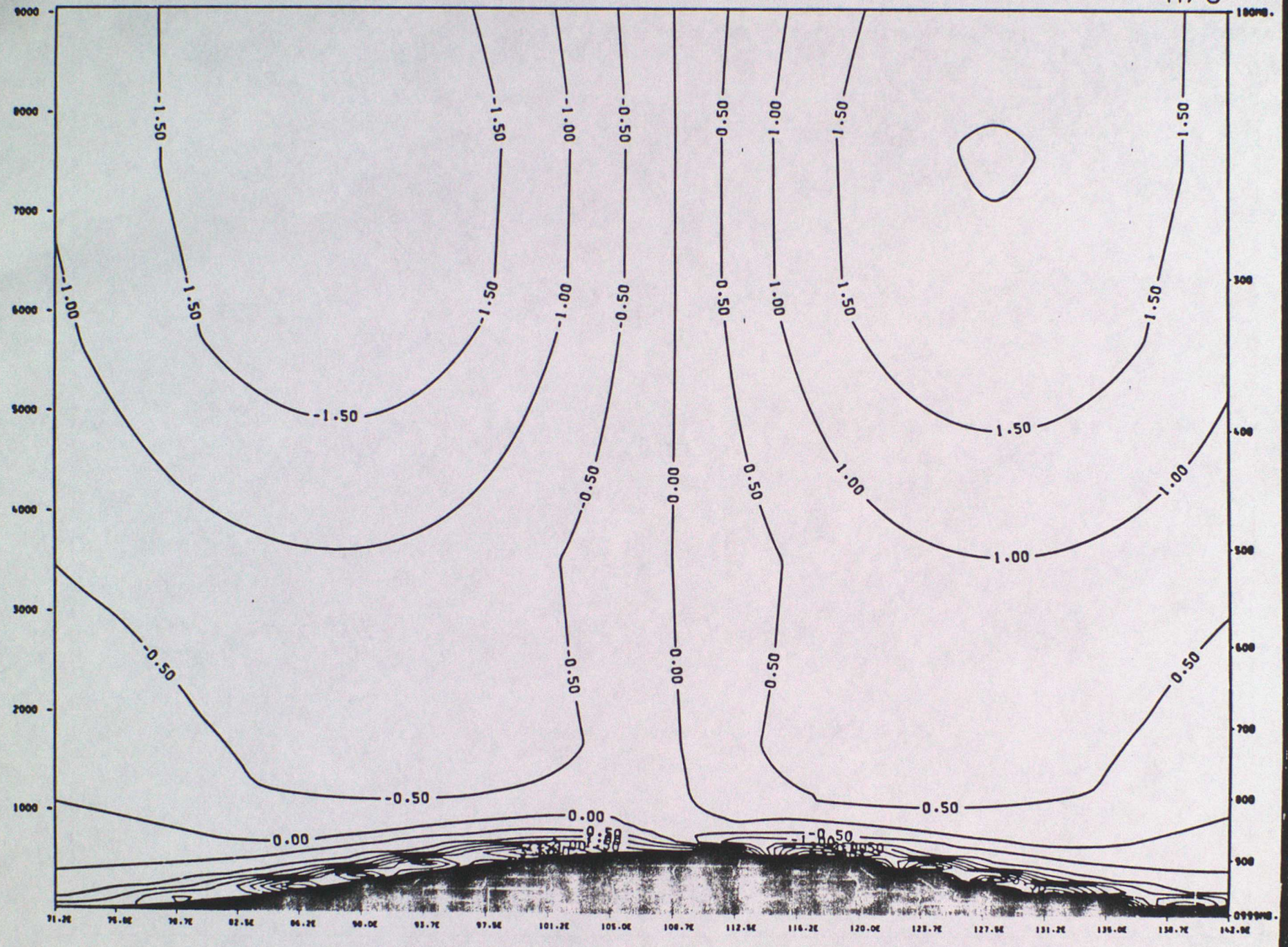

CROSS-SECTION ALONG LATITUDE 45.00N

Figure. 1.

U COMPONENT OF WIND

M/S

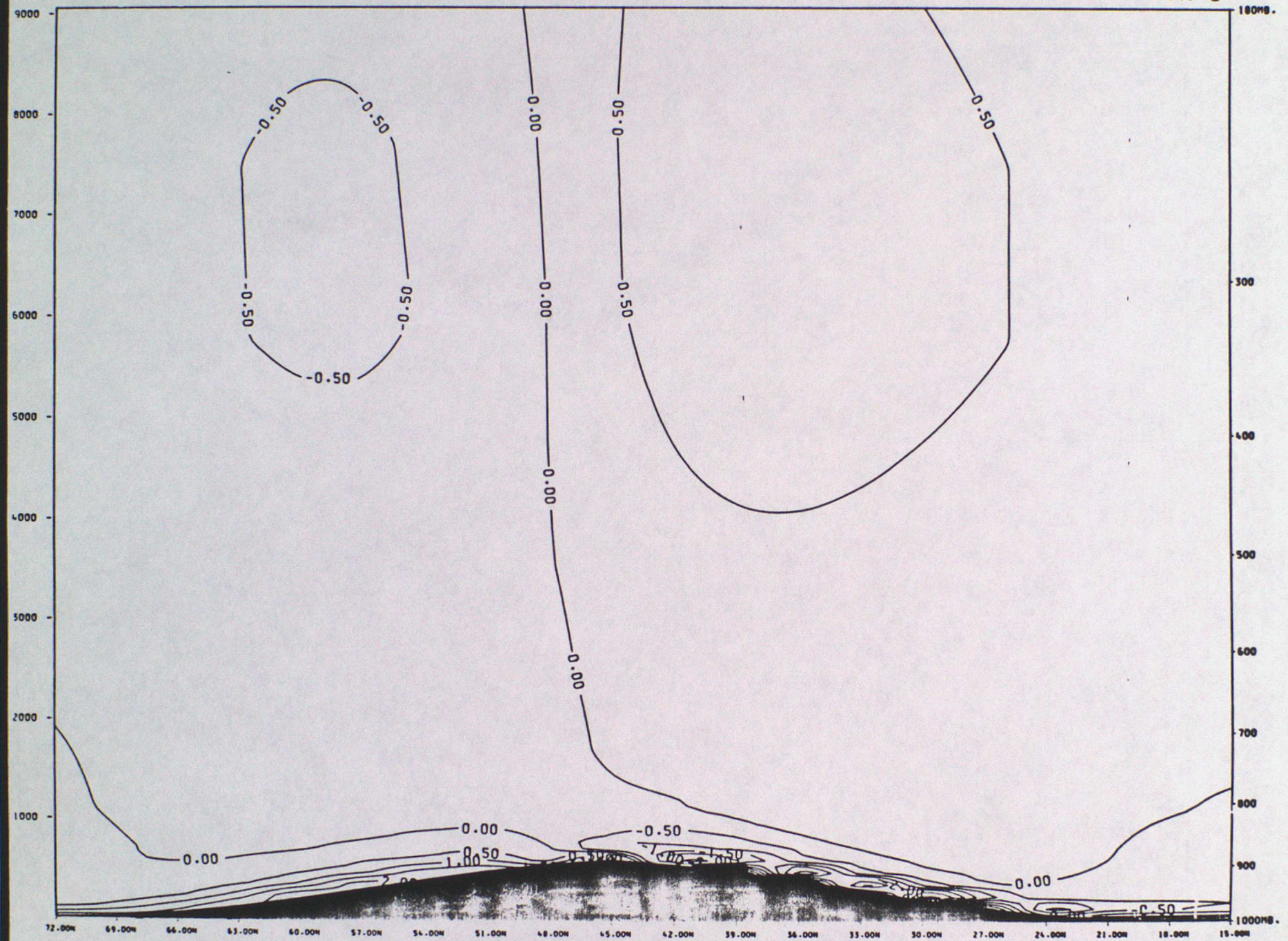

CROSS-SECTION ALONG LONGITUDE 108.75E

Figure 10

V_g COMPONENT OF WIND

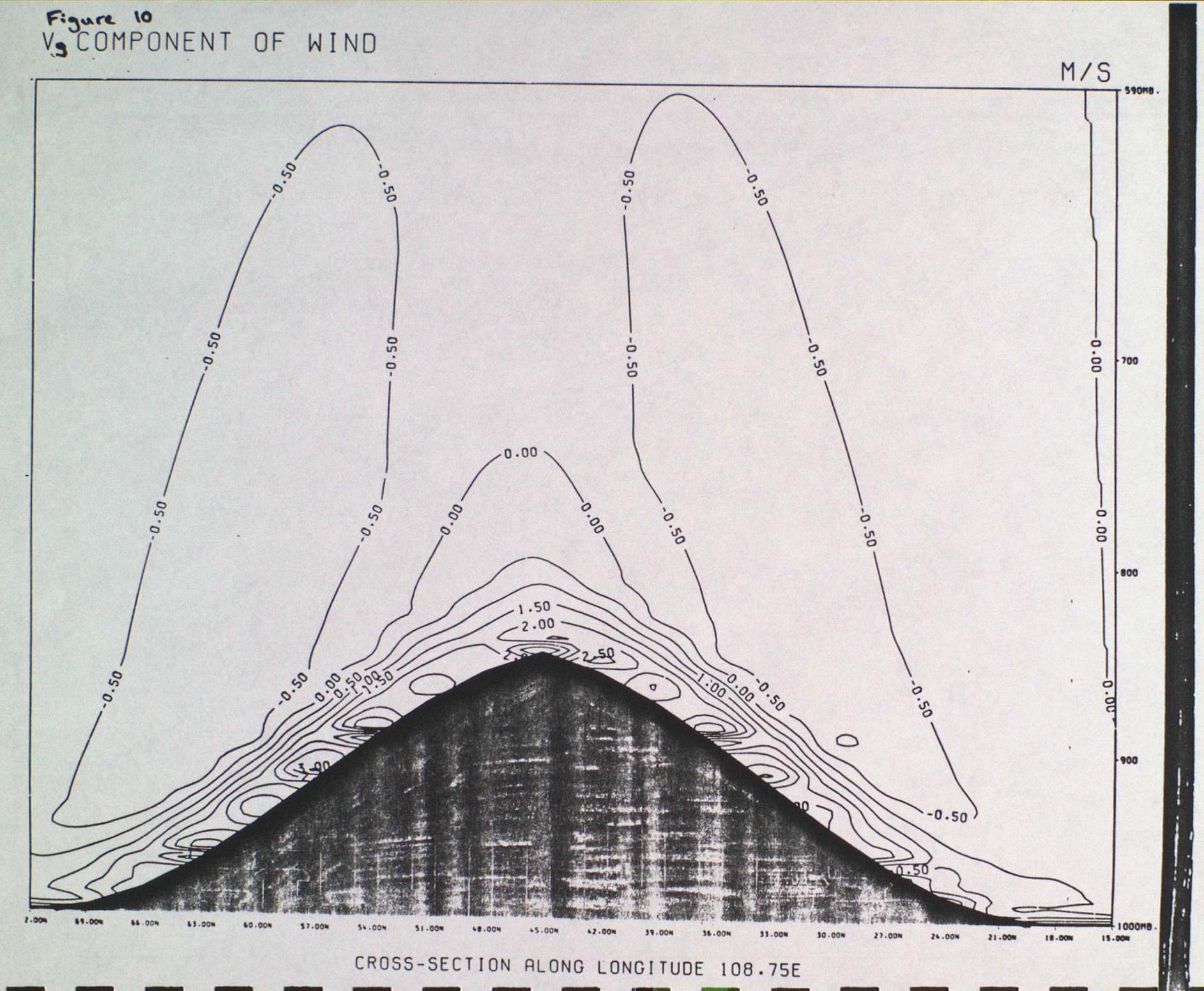

CROSS-SECTION ALONG LONGITUDE 108.75E

Figure 11.

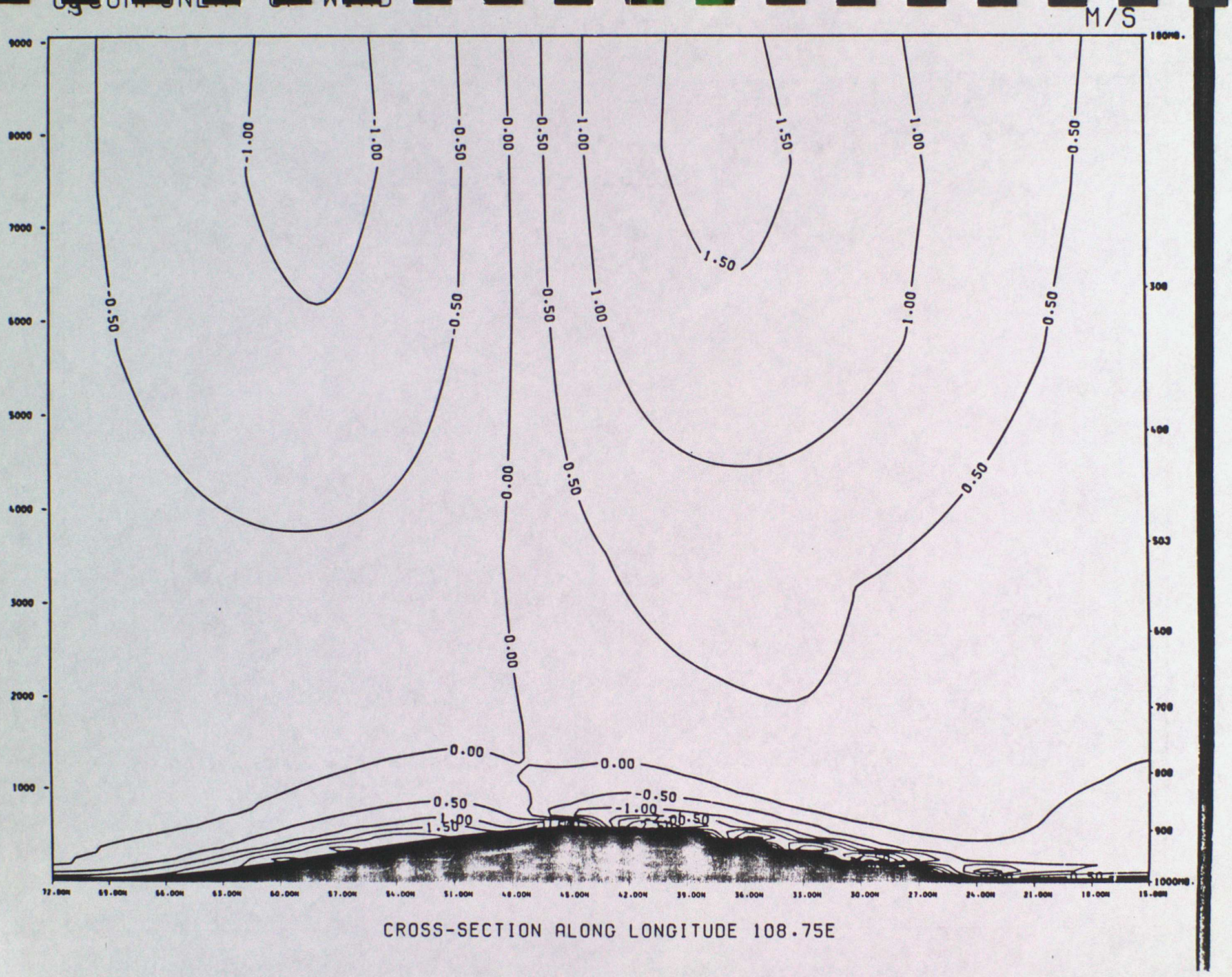

CROSS-SECTION ALONG LONGITUDE 108.75E

Figure 12.

V_g COMPONENT OF WIND

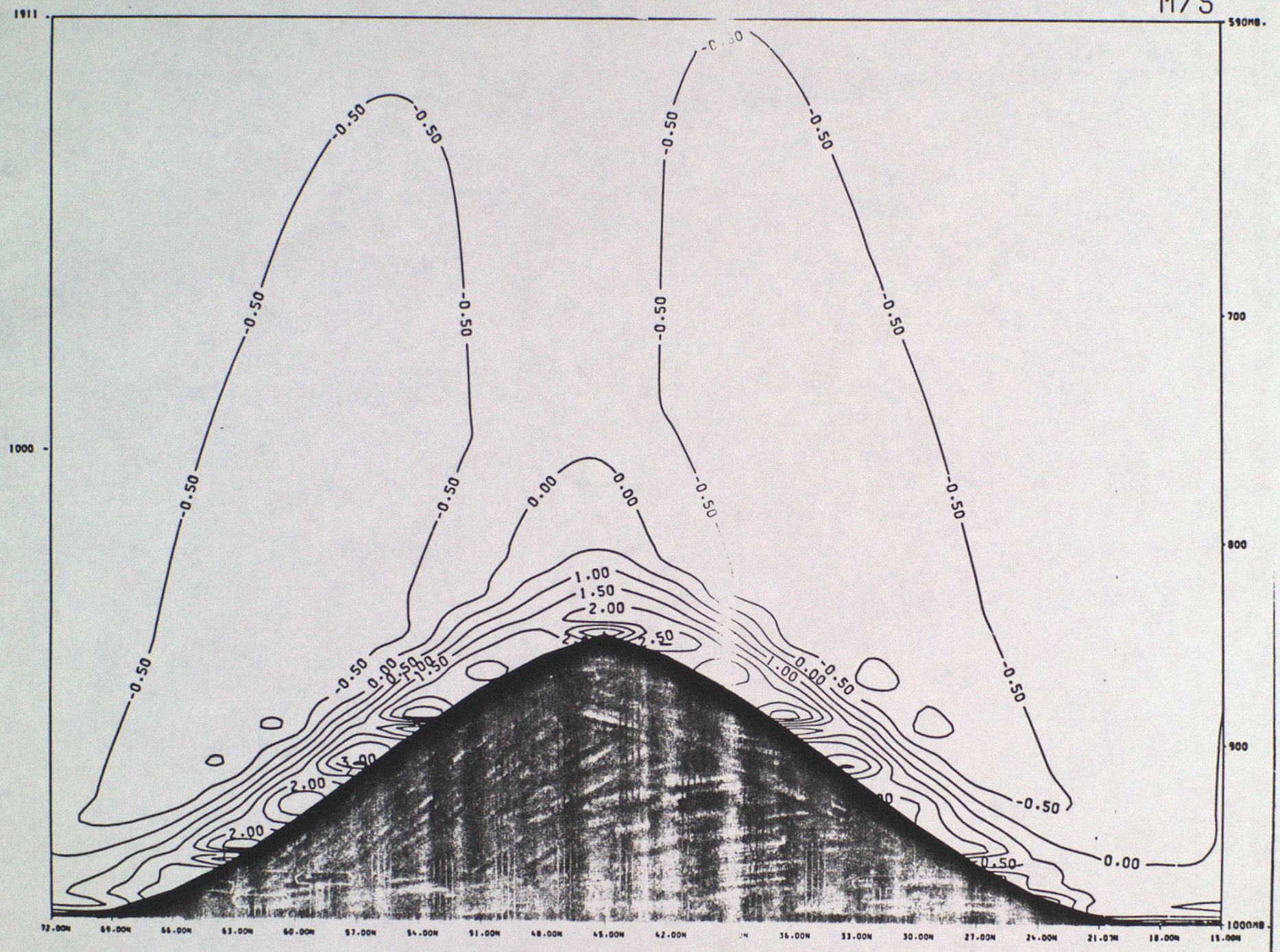

CROSS-SECTION ALONG LONGITUDE 108.75E

Figure 13.

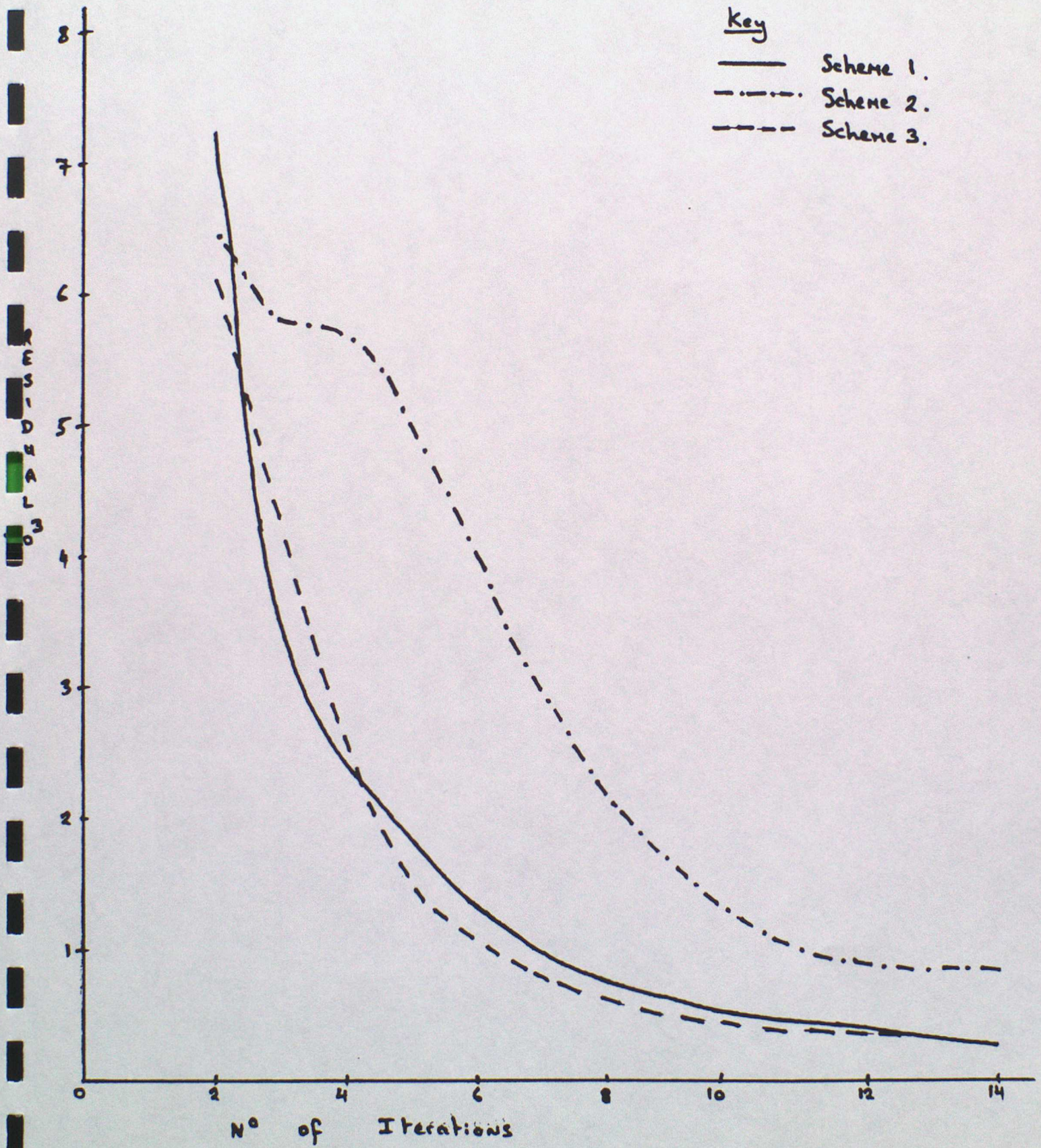
Key
Scheme 1.
Scheme 2.
Scheme 3.
RESIDUALS
8
7
6
5
4
3
2
1
0
2
4
6
8
10
12
14
N° of Iterations